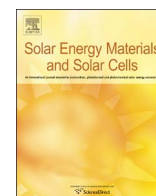




ELSEVIER

Contents lists available at ScienceDirect

Solar Energy Materials & Solar Cells

journal homepage: www.elsevier.com/locate/solmat

Compact and high-power dye-sensitized solar system integrated with low-cost solar-concentrating polymer lens



Sung-Hun Ha^a, Hyun-Woo Yu^a, Nam-Su Jang^a, Ji Hoon Kim^a, Soo-Hyung Kim^{a,b,*}, Jong-Man Kim^{a,b,*}

^a Department of Nano Fusion Technology and BK21 Plus Nano Convergence Technology Division, Pusan National University, Busan 609-735, Republic of Korea

^b Department of Nanoenergy Engineering, Pusan National University, Busan 609-735, Republic of Korea

ARTICLE INFO

Article history:

Received 17 February 2016

Received in revised form

10 June 2016

Accepted 16 June 2016

Keywords:

Polymer lens

Low-cost

Compact structure

High-power solar system

Self-cleaning

ABSTRACT

A dye-sensitized solar cell (DSSC) is integrated monolithically with a polymer lens to demonstrate a compact, low-cost and high-power solar energy harvesting system. The proposed polymer lens is composed of a plano-convex lens for concentrating light and a supporting layer for controlling the distance between the lens and DSSC according to its thickness. A single-step polymer replication process with a glass-based lens mold makes it possible to fabricate the polymer lens in a simple and reproducible manner. The power conversion performance of the polymer lens-integrated dye-sensitized (PLD) solar system is optimized by simply controlling the height of the supporting layer. The maximum output power of DSSC is improved by ~50.2% after monolithically integrating with the polymer lens with a 3-mm-thick supporting layer. Finally, the PLD solar system is packaged with a self-cleanable polymer film to protect the lens from the environment and to make the system robust to contamination. Through a simple self-cleaning test, it is found that the PLD system can recover ~95.2% of its original output power.

© 2016 Elsevier B.V. All rights reserved.

1. Introduction

A high price-to-performance ratio is one of the most crucial factors that should be considered in developing solar energy harvesters. To achieve this, many efforts have been made over the past decades to enhance the light-to-power conversion performance of dye-sensitized solar cells (DSSCs), which have superior cost-effectiveness in manufacturing compared to other semiconductor cells [1–8]. To date, extensive research on the development of new materials and architectures for DSSCs has resulted in steady enhancement of output power [9–16]. In addition to the approaches, a multifunctional luminescent fluoropolymer coating has been introduced to improve power conversion efficiency and long-term stability of DSSCs [17,18]. Optical lenses can also be integrated with DSSCs to enhance the output power by directly concentrating the sunlight onto the photoactive electrodes [19–21]. This approach makes it possible to increase the output power of DSSCs efficiently and is potentially feasible for further enhancement of the output power when combined with material and structural strategies [21]. However, lens-integrated solar

systems inevitably become bulky and complicated because several mechanical parts must also be integrated into the system to physically support the lens, as well as to control the focal length by adjusting the distance between the lens and solar cell. Furthermore, the use of expensive glass-based lenses significantly increases the overall manufacturing cost of integrated solar systems. These issues critically hinder applications in various fields that require high-power, compact, and cost-effective solar energy harvesters.

This work demonstrates a low-cost polymer lens that can potentially be employed as a solar-concentrating device for developing a compact and high-power dye-sensitized solar system. The polymer lens was simply prepared from a glass-based lens mold through a standard polydimethylsiloxane (PDMS) replication process. The lens was monolithically integrated with a DSSC by bonding it onto the top surface. There are several advantages of the polymer lens-integrated dye-sensitized (PLD) solar system compared to conventional lens-integrated solar systems as follows. First, the overall manufacturing cost can be dramatically reduced by replacing expensive glass-based lenses with low-cost polymer ones while maintaining fair optical performance due to the high transparency of PDMS. Second, compact architecture is highly achievable because the polymer lens can be monolithically integrated with a DSSC, and the system performance can be easily controlled by adjusting the thickness of the lens structure without any mechanical parts. Finally, the polymer

* Corresponding authors at: Department of Nano Fusion Technology and BK21 Plus Nano Convergence Technology Division, Pusan National University, Busan 609-735, Republic of Korea.

E-mail addresses: sookim@pusan.ac.kr (S.-H. Kim), jongkim@pusan.ac.kr (J.-M. Kim).

lens is very robust to dust contamination, physical damages, and self-cleanable because the lens is fully packaged with a self-cleanable PDMS film.

2. Experimental details

2.1. Fabrication of polymer lens and self-cleanable film

The polymer lens and self-cleanable film were simply prepared by a PDMS replication process. For fabrication of the polymer lens, a plano-concave glass-based lens (Edmund Optics) was placed inside a plastic container and used as a mold. The diameter, edge thickness, and center thickness of the plano-concave lens are 8.4, 3.63, and 2.25 mm, respectively. A PDMS prepolymer (Sylgard 184 A, Dow Corning) mixed with a curing agent (Sylgard 184 B, Dow Corning) at a weight ratio of 10:1 was poured into the container, followed by thermal curing in a convection oven at 70 °C for 1 h. The polymer lens was finally prepared by peeling it off from the mold.

For fabrication of the self-cleanable PDMS film, a ~ 70 - μm -thick photoresist layer (PR, JSR THB-151N; JSR Micro) with square holes was periodically patterned on a silicon substrate using a photolithographic process. The PDMS/curing-agent mixture (at a weight ratio of 10:1) was then spin-coated onto the mold substrate at 500 rpm for 30 s and then cured at 70 °C for 1 h. The micropillar-arrayed PDMS film was carefully peeled off from the mold substrate and coated conformally with a thin fluorocarbon (FC) layer using a chemical vapor deposition (CVD) method to decrease the surface energy.

2.2. Fabrication of DSSC

DSSCs were fabricated using guidelines from previous studies [20,22]. Commercially available TiO_2 nanoparticles (NPs) were purchased (P25, Degussa, Sigma-Aldrich) and used without further treatment. The photoactive electrode was a screen-printed TiO_2 thin film on fluorine-doped tin oxide (FTO) glass ($\text{SnO}_2\cdot\text{F}$, $7 \Omega/\text{sq}$, Pilkington) with a photoactive area of $0.6 \times 0.6 \text{ cm}^2$. Briefly, TiO_2 NPs-based paste was prepared for screen printing process by mixing 6 g of TiO_2 NPs, 15 g of ethanol, 1 mL of acetic acid (CH_3COOH), and 20 g of terpineol in a vial and sonicating for 1 h. A solution of 3 g of ethylcellulose dissolved in 27 g of ethanol was also prepared and mixed with the TiO_2 NP-dispersed solution and sonicated for 30 min.

The resulting TiO_2 paste was screen-printed on FTO glass pretreated with a solution of 0.247 mL of TiOCl_2 and 20 mL of deionized water to enhance the adhesion between the TiO_2 thin films. The TiO_2 thin film on the FTO glass was then sintered in an electric furnace at 500 °C for 30 min and immersed in anhydrous ethanol containing 0.3 mM of Ru-dye (Bu_4N) $_2$ [Ru(Hdcbpy) $_2$ -(NCS) $_2$] (N719 dye, Solaronix) for 24 h at room temperature for adsorption of dye molecules on the surface of the TiO_2 thin films. The dye-soaked TiO_2 photoactive electrode was then rinsed with ethanol and dried in a convection oven at 80 °C for 10 min.

Pt-coated FTO glass was prepared by ion sputtering (E1010, Hitachi) at 2.5 kV and used as a counter electrode. Both the dye-adsorbed TiO_2 photoactive electrode and the Pt-coated counter electrode were assembled into a sandwich-type structure with a 60- μm -thick hot-melt polymer film (Surlyn, DuPont) as a spacer. The internal space between the electrodes was then filled with an iodide-based liquid electrolyte (AN-50, Solaronix).

2.3. Characterization

Isotropic and cross-sectional images of the fabricated polymer lens and PLD solar system were obtained with a digital camera. The

2D surface and cross-sectional profiles of the glass-based lens mold and polymer lens were observed using a laser interferometer (NV-1000, Nanosystem). The detailed surface morphology of the fabricated polymer lens was measured using an atomic force microscope (AFM; NX10, Park Systems) in non-contact mode. The surface geometry of the fabricated self-cleanable film was observed using an optical microscope (BX60M, Olympus) and laser interferometer.

The surface wetting property of the self-cleanable film was evaluated by characterizing the static contact angle (SCA) and contact angle hysteresis (CAH) using a contact angle meter (DSA 20E, KRÜSS) equipped with a CCD camera module. The optical property of the self-cleanable film was characterized by measuring the optical transmittance at wavelengths ranging from 400 to 800 nm with an air baseline using UV-visible spectroscopy (S310, SCINCO).

The power conversion performance of the PLD solar system was evaluated by characterizing the output power density under AM 1.5 simulated illumination with an intensity of $100 \text{ mW}/\text{cm}^2$ using a commercially available solar simulator (PEC-L11, Peccell Technologies). The output power density (P_o) can be defined as $P_o = J_{sc} \times V_{oc} \times FF$, where J_{sc} , V_{oc} , and FF are short-circuit current density, open-circuit voltage, and fill factor, respectively. The measurements were performed on at least three systems for each model with different heights of the supporting PDMS.

The self-cleaning performance of the PLD solar system was characterized by comparing the output power densities of the system in initial, contaminated, and cleaned states. The PLD solar system was contaminated by randomly scattering alumina microparticles onto the top surface and cleaned by introducing several water droplets onto the contaminated surface at an inclination of $\sim 10^\circ$.

3. Results and discussion

Fig. 1(a) shows a schematic illustration of the PLD solar system under light illumination. The polymer lens consists of the plano-convex lens and supporting PDMS parts and it is monolithically integrated onto the top surface of the DSSC. The lens part plays a role in concentrating the incident light and focusing it onto the photoactive electrode of the DSSC. The light-to-electricity power output of the PLD solar system can be optimized easily by controlling the height (h_s) of the supporting PDMS. This is because the circular area of light focused onto the photoactive electrode is determined by the distance between the lens and the DSSC.

Fig. 1(b) shows the calculated radius of the focused light area (R_f) as a function of h_s of up to 5 mm. The details for the calculation are described in Fig. S1 in the Supporting Information (SI). When increasing h_s , the circular area of focused light becomes smaller due to a gradual decrease of R_f . This indicates that the incident light is more densely concentrated onto the photoactive electrode with a fixed area of $0.6 \times 0.6 \text{ cm}^2$ (an increase in the utilization rate of the focused light area), while the utilization rate of the photoactive electrode is accordingly decreased, as shown in the inset of Fig. 1(b) and Fig. S2 in the SI. This also suggests that the power conversion performance of the PLD solar system can be systematically optimized by controlling h_s to mediate between the two contradictory factors (the utilization rates of the focused light area and the photoactive electrode). To estimate effect of h_s on the power conversion performance of the PLD solar system, the calculated utilization rates of the focused light area and photoactive electrode were averaged while varying the weighting of the two factors, as shown in Fig. S3 in the SI. Assuming that the two factors predominantly determine the performance of the PLD solar system, h_s can be designed to achieve maximum performance at the highest average utilization rates, as shown in Table S1.

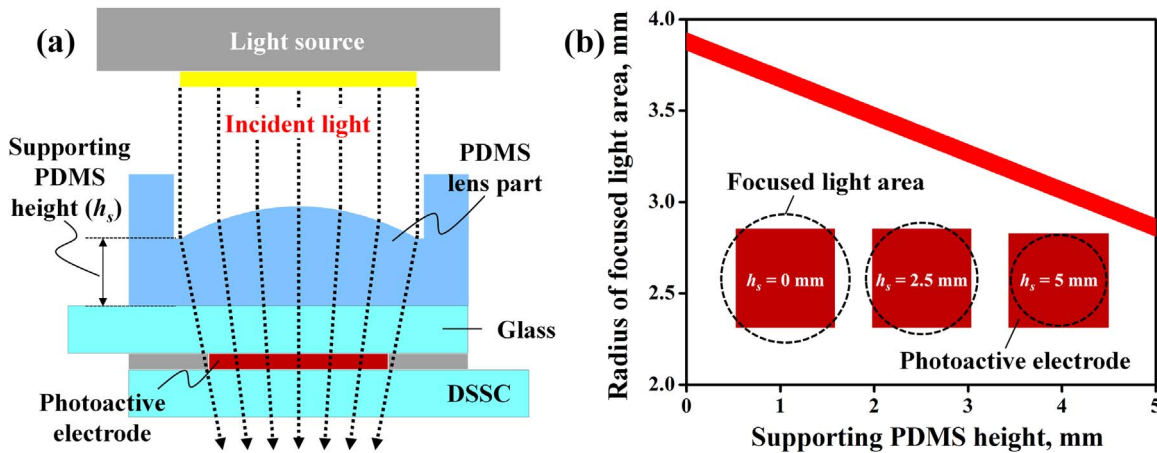


Fig. 1. Polymer lens-integrated dye-sensitized (PLD) solar system. (a) Schematic illustration of the PLD solar system under light illumination. (b) Calculated radius of focused light area as a function of supporting PDMS height up to 5 mm (inset: schematic illustration of circular area of light focused onto photoactive electrode with a fixed area of $0.6 \times 0.6 \text{ cm}^2$).

The polymer lens fabricated by the PDMS replication process is illustrated schematically in Fig. 2(a). Fig. 2(b) shows digital images of the fabricated plano-convex polymer lens with simple architecture and a smooth surface. Fig. 2(c) and Fig. S4 in the SI show the 2D surface and cross-sectional profiles (y -axis: A-A', x -axis: B-B') measured in the center regions of the glass-based lens mold and polymer lens. The concave surface of the lens mold was almost perfectly replicated in the convex surface on the polymer lens without significant shape discrepancy. Importantly, the AFM topographic profiles in Fig. 2(d) clearly show that the polymer lens surface is very smooth with surface roughness (R_a) as low as $\sim 3.1 \text{ nm}$. These results clearly demonstrate that the PDMS replication process is highly suitable for the fabrication of a solar-concentrating lens that ensures cost-effectiveness, simplicity in manufacturing, and potentially high optical performance due to the smooth surface. h_s was determined by simply calculating the required mass of the PDMS mixture to achieve the necessary height with respect to fixed dimensions of the container.

Fig. 2(e) shows h_s measured as a function of the mass of the PDMS mixture with negligible errors compared to the calculated values. Notably, the issue of curing-induced shrinkage of the PDMS would be insignificant in this size regime [23]. This also suggests that h_s can be precisely controlled by changing the mass of the PDMS mixture, resulting in a precise optimization of the light-to-electricity conversion performance of the PLD solar system.

The digital image of the fabricated PLD solar system in Fig. 3(a) clearly shows compact architecture without any mechanical parts for both supporting the lens and changing the distance between the lens and DSSC. Fig. 3(b) shows digital images of the PLD solar system under light illumination in a solar simulator. All the PLD solar systems were tested under the same conditions except for h_s of the polymer lens. Fig. 3(c) shows the rate of increase in P_o (r_p) of the PLD solar system according to h_s values ranging from 1.8 mm to 3.4 mm with a step of 0.4 mm. The change in h_s affects r_p by simultaneously changing two factors: (1) the circular area of light focused onto the photoactive electrode and (2) the effective photoactive area activated by the incident light, as described in Fig. 1(b). r_p gradually increased with h_s up to 3 mm, as shown in Fig. 3(c). This probably resulted from the focused light increasing the photoreaction on the photoactive electrode, although the effective electrode area activated by the focused light is decreased. However, although the light becomes more focused even when h_s exceeds 3 mm, r_p was reduced. This means that the photoreaction is critically limited to a small area on the photoactive electrode (a large decrease in the utilization rate of the

photoactive electrode), which was due to excessive concentration of light, resulting in a decrease in r_p . In particular, the rate of increase in J_{sc} of the PLD solar system according to h_s was very close to r_p , as shown in Fig. 3(b) and S5 in the SI. This suggests that P_o of the system is determined depending predominantly on J_{sc} that is generated by the photoreaction on the photoactive electrode with the concentrated light.

The output power density of the PLD solar system was improved by $\sim 50.2\%$ compared to that of the bare DSSC when R_l was optimized to $\sim 3.27 \text{ mm}$ at $h_s = 3 \text{ mm}$, corresponding to $\sim 50.9\%$ increase in J_{sc} . Comparing the estimation in Fig. S3 and Table S1 indicated that the experimental results are consistent with the calculated ones when the weighting ratio of the two factors is 1:1 ($R_l = \sim 3.26 \text{ mm}$ at $h_s = \sim 3.06 \text{ mm}$). This suggests that the utilization rates of the focused light area and photoactive electrode evenly affect the power conversion performance of the PLD solar system because the two factors were simply averaged in the calculation while disregarding weighting.

Fig. 3(c) also shows that the values of r_p of the PLD solar systems are quite uniform with small deviations for each model, even though the systems were fabricated separately. This is mainly attributed to (1) the optical transparency of PDMS making it easy for the polymer lens to be integrated with the DSSC while ensuring good alignment and (2) the polymer lens fabrication being quite reproducible because it is based on the well-established PDMS replication process.

Fig. 4(a) shows a digital image of the PLD solar system packaged with a self-cleanable PDMS film and the surface morphology of the film. The packaged system was simply made by intimately bonding the micro-pillar-arrayed PDMS film onto the polymer lens. The height and width of the micro-pillar and inter-pillar (edge-to-edge) distance on the PDMS film are $\sim 70 \mu\text{m}$, $\sim 120 \mu\text{m}$, and $\sim 150 \mu\text{m}$, respectively, as shown in the optical microscope and 3D profiling images of Fig. 4(a). It is important to achieve high SCA and low CAH of the PDMS film so that water droplets can easily roll off from the surface while washing off dust particles, resulting in self-cleaning property of the polymer lens. Fig. 4(b) shows the surface wetting properties of the fabricated PDMS film. SCA and CAH were measured as $146.5 \pm 2.2^\circ$ and $11.7 \pm 0.4^\circ$, respectively, which implies that the PDMS film is hydrophobic enough to produce the self-cleaning effect. The fabricated PDMS film is also optically transparent with a high transmittance of $\sim 84.6\%$ at a wavelength of 550 nm, as shown in Fig. 4(c). This desirable performance mainly originates from the suitable surface design with relatively large inter-pillar distance. The large spaces

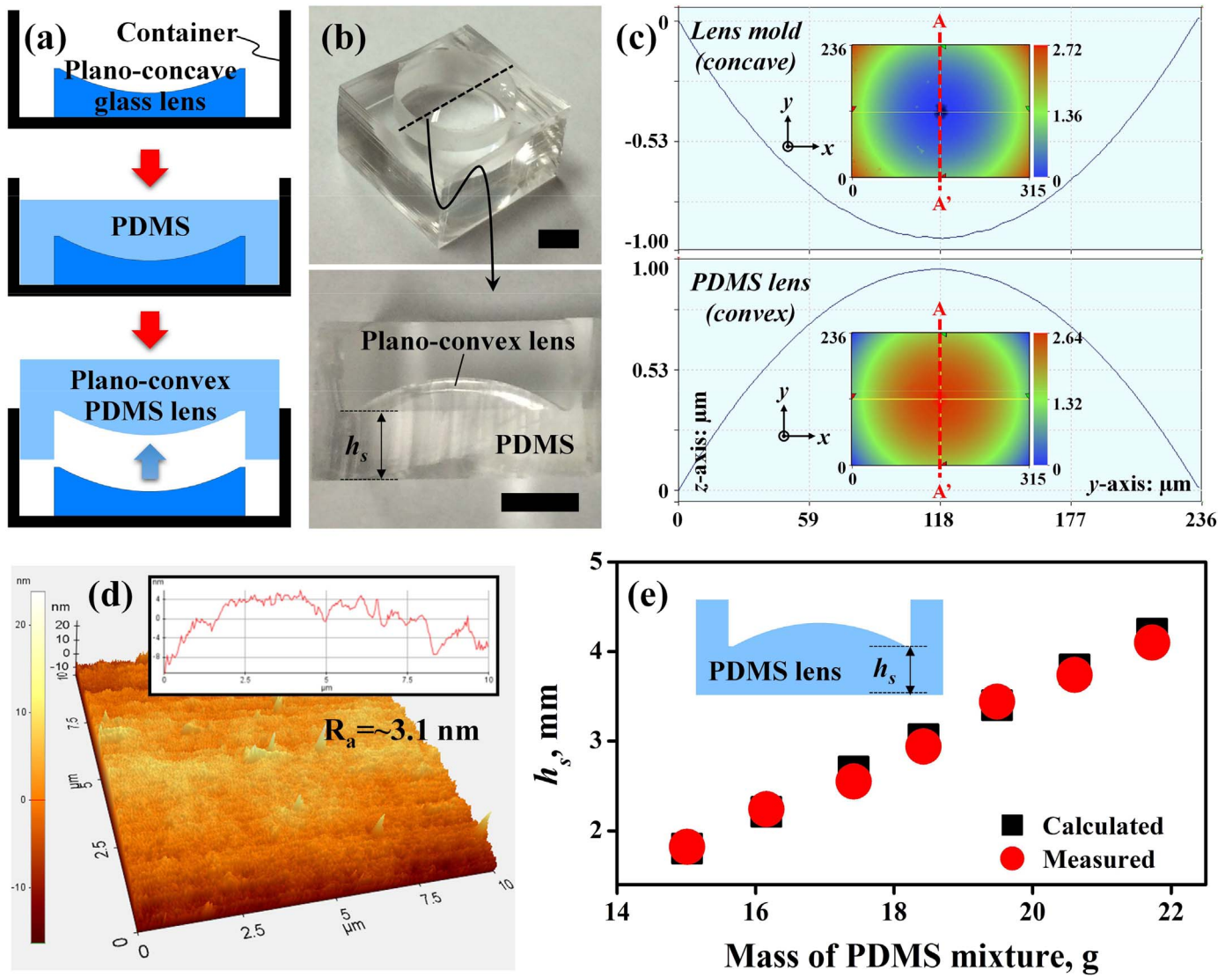


Fig. 2. Fabrication of solar-concentrating polymer lens. (a) Schematic illustration of the fabrication for polymer lens. (b) Digital images of the fabricated polymer lens (scale bars: 3 mm). (c) 2D surface and cross-sectional (A-A') profiles measured in center regions of the glass-based lens mold and polymer lens (laser-scanned area: $315 \mu\text{m} \times 236 \mu\text{m}$). (d) AFM topographic profiles of polymer lens surface (scanned area: $10 \mu\text{m} \times 10 \mu\text{m}$, inset: cross-sectional line profile). (e) Measured and calculated supporting PDMS heights as a function of the mass of the PDMS mixture (inset: schematic illustration of polymer lens).

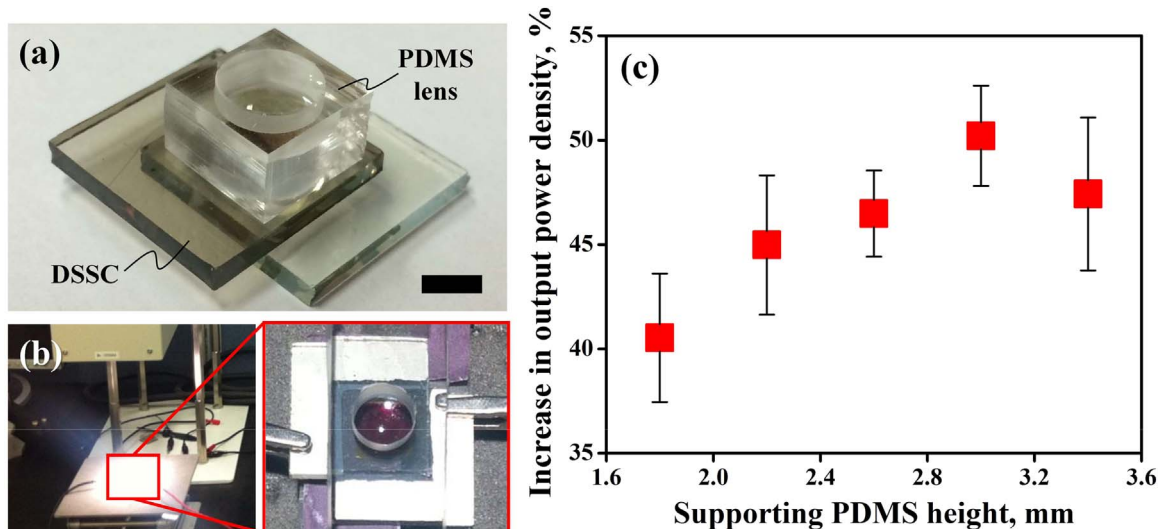


Fig. 3. Power conversion performance of the PLD solar system. Digital images of (a) fabricated PLD solar system (scale bar: 5 mm) and (b) measurement setup. (c) Rate of increase in output power density of the PLD solar system as a function of supporting PDMS height.

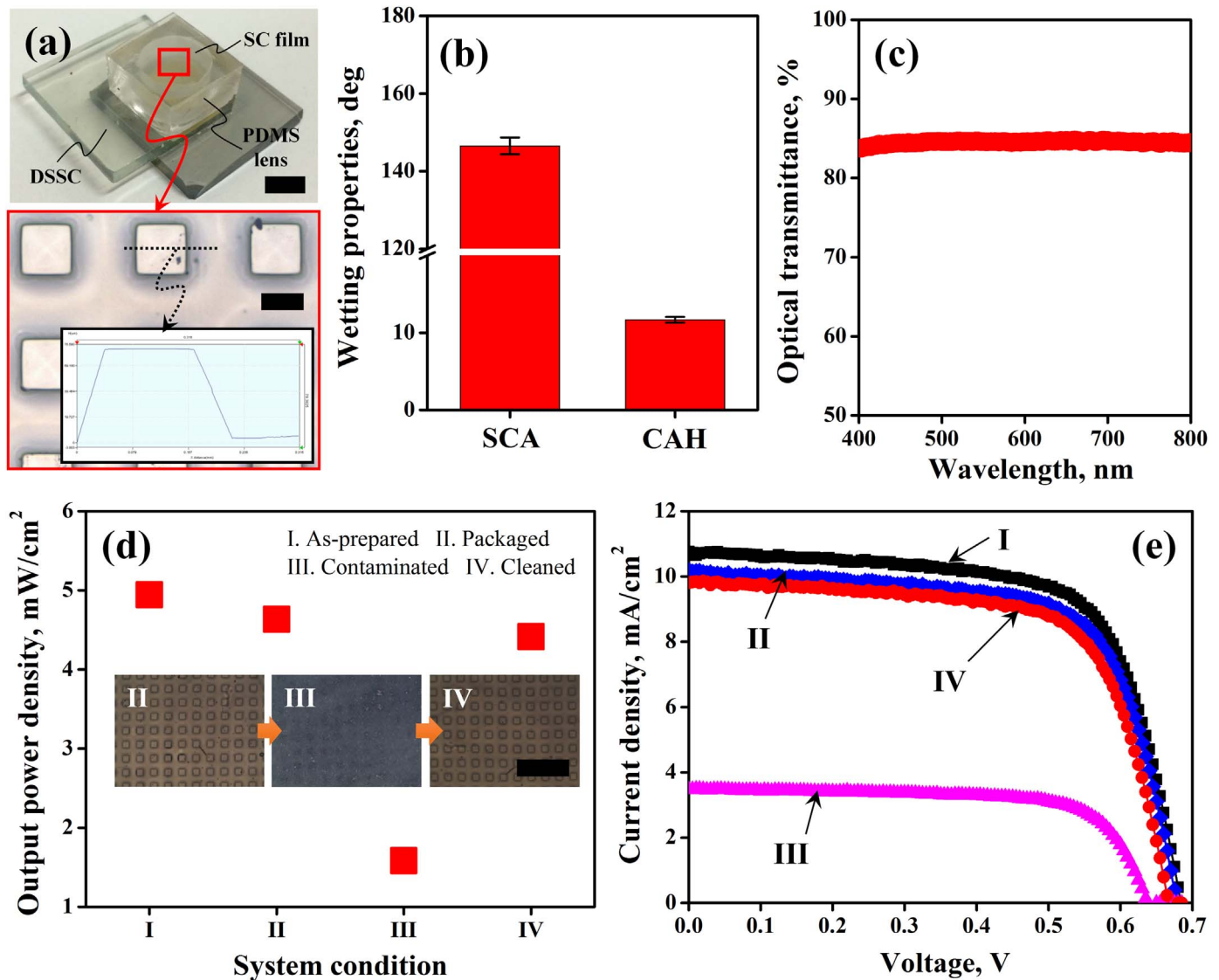


Fig. 4. PLD solar system packaged with a self-cleanable PDMS film. (a) Digital image of the packaged PLD solar system (upper scale bar: 5 mm) and detailed surface morphologies of the self-cleanable film (lower scale bar: 100 μm). (b) Surface wetting properties (SCA and CAH) and (c) optical transmittance curve of the fabricated self-cleanable film. (d) The values of P_o and (e) J - V curves of the packaged PLD solar system for three different conditions: as-prepared, contaminated, and cleaned (inset: microscope images of the self-cleanable film for three different conditions, scale bar: 1 mm).

between the micro-pillars provide sufficient air-pocket sites that can prevent surface wetting and allow light to pass through without appreciable scattering effect [24].

Fig. 4(d) and (e) show the values of P_o and current density-voltage (J - V) curves measured for the packaged PLD solar system in three different states: as-prepared, contaminated, and cleaned. The self-cleaning test was carried out using the PLD solar system with an initial P_o of $\sim 4.94 \text{ mW/cm}^2$. After packaging with the self-cleanable PDMS film, P_o of the system slightly decreased to $\sim 4.64 \text{ mW/cm}^2$, probably due to the loss of light passing through the micro-roughened PDMS film. P_o of the system was sharply degraded to $\sim 1.58 \text{ mW/cm}^2$ after contamination with alumina particles. However, the power conversion performance of the system easily recovered to $\sim 4.41 \text{ mW/cm}^2$ after the self-cleaning test, which corresponds to $\sim 95.2\%$ recovery with respect to the packaged PLD solar system in the initial state.

Fig. 4(e) clearly indicates that P_o of the packaged PLD solar system was predominantly affected by the change in J_{sc} rather than V_{oc} and FF during the self-cleaning test. This supports that alumina particles scattered randomly on the top surface led to a steep

decrease in J_{sc} (from $\sim 9.96 \text{ mA/cm}^2$ to $\sim 3.42 \text{ mA/cm}^2$) by hindering light transmission through the PDMS film [25,26]. However, J_{sc} almost returned to its original value (from $\sim 3.42 \text{ mA/cm}^2$ to $\sim 9.68 \text{ mA/cm}^2$) after removing most of the alumina particles through the simple self-cleaning process. This suggests that the simple packaging approach would be greatly helpful for protecting the polymer lens from the operation environment and preventing the solar system from being degraded by contamination.

4. Conclusion

This work demonstrated a compact dye-sensitized solar system integrated monolithically with a low-cost solar-concentrating polymer lens for enhancing the output power of conventional DSSCs. The polymer lenses were easily and reproducibly fabricated by a PDMS replication process with a glass-based lens mold. The maximum output power of the PLD solar system was improved by $\sim 50.2\%$ compared to the as-prepared DSSC when the supporting PDMS height was optimized to 3 mm. The PLD solar system also

had superior self-cleaning properties after being packaged with a micro-pillar-arrayed PDMS film, which had a high SCA of $146.5 \pm 2.2^\circ$ and low CAH of $11.7 \pm 0.4^\circ$. A PLD solar system that was severely contaminated with alumina particles recovered $\sim 95.2\%$ of its original output power density after the simple cleaning process. The packaged PLD solar systems could have many practical applications due to advantages that include compact architecture, simplicity and cost-effectiveness in manufacturing, robustness to the environment and contamination, and enhanced power conversion performance.

Acknowledgement

This work was supported by a 2-Year research Grant of Pusan National University, South Korea.

Appendix A. Supplementary material

Supplementary data associated with this article can be found in the online version at <http://dx.doi.org/10.1016/j.solmat.2016.06.038>.

References

- [1] M.R. Narayan, Review: dye sensitized solar cells based on natural photosensitizers, *Renew. Sustain. Energy Rev.* 16 (2012) 208–215.
- [2] B.E. Hardin, H.J. Snaith, M.D. McGehee, The renaissance of dye-sensitized solar cells, *Nat. Photonics* 6 (2012) 162–169.
- [3] A. Hagfeldt, G. Boschloo, L. Sun, L. Kloo, H. Pettersson, Dye-sensitized solar cells, *Chem. Rev.* 110 (2010) 6595–6663.
- [4] J.-H. Yum, P. Chen, M. Grätzel, M.K. Nazeeruddin, Recent developments in solid-state dye-sensitized solar cells, *ChemSusChem* 1 (2008) 699–707.
- [5] S. Zhang, X. Yang, Y. Numata, L. Han, Highly efficient dye-sensitized solar cells: progress and future challenges, *Energy Environ. Sci.* 6 (2013) 1443–1464.
- [6] M. Ye, X. Wen, M. Wang, J. Iocozzia, N. Zhang, C. Lin, Z. Lin, Recent advances in dye-sensitized solar cells: from photoanodes, sensitizers and electrolytes to counter electrodes, *Mater. Today* 18 (2015) 155–162.
- [7] H. Hug, M. Bader, P. Mair, T. Glatzel, Biophotovoltaics: natural pigments in dye-sensitized solar cells, *Appl. Energy* 115 (2014) 216–225.
- [8] Md.K. Nazeeruddin, E. Baranoff, M. Grätzel, Dye-sensitized solar cells: a brief overview, *Sol. Energy* 85 (2011) 1172–1178.
- [9] S. Mathew, A. Yella, P. Gao, R. Humphry-Baker, B.F.E. Curchod, N. Ashari-Astani, I. Tavernelli, U. Rothlisberger, Md.K. Nazeeruddin, M. Grätzel, Dye-sensitized solar cells with 13% efficiency achieved through the molecular engineering of porphyrin sensitizers, *Nat. Chem.* 6 (2014) 242–247.
- [10] M. Peng, S. Hou, H. Wu, Q. Yang, X. Cai, X. Yu, K. Yan, H. Hu, F. Zhu, D. Zou, Integration of fiber dye-sensitized solar cells with luminescent solar concentrators for high power output, *J. Mater. Chem. A* 2 (2014) 926–932.
- [11] Z. Yao, M. Zhang, H. Wu, L. Yang, R. Li, P. Wang, Donor/acceptor indenoperylene dye for highly efficient organic dye-sensitized solar cells, *J. Am. Chem. Soc.* 137 (2015) 3799–3802.
- [12] N. Zhou, K. Prabakaran, B. Lee, S.H. Chang, B. Harutyunyan, P. Guo, M.R. Butler, A. Timalisina, M.J. Bedzyk, M.A. Ratner, S. Vegiraju, S. Yau, C.-G. Wu, R.P. H. Chang, A. Facchetti, M.-C. Chen, T.J. Marks, Metal-free tetrathienoacene sensitizers for high-performance dye-sensitized solar cells, *J. Am. Chem. Soc.* 137 (2015) 4414–4423.
- [13] Q. Wang, S. Ito, M. Grätzel, F. Fabregat-Santiago, I. Mora-Seró, J. Bisquert, T. Bessho, H. Imai, Characteristics of high efficiency dye-sensitized solar cells, *J. Phys. Chem. B* 110 (2006) 25210–25221.
- [14] T. Daeneke, T.-H. Kwon, A.B. Holms, N.W. Duffy, U. Bach, L. Spiccia, High-efficiency dye-sensitized solar cells with ferrocene-based electrolytes, *Nat. Chem.* 3 (2011) 211–215.
- [15] L. Han, A. Islam, H. Chen, C. Malapaka, B. Chiranjeevi, S. Zhang, X. Yang, M. Yanagida, High-efficiency dye-sensitized solar cell with a novel co-adsorbent, *Energy Environ. Sci.* 5 (2012) 6057–6060.
- [16] U.O. Krašovec, M. Berginc, M. Hočevar, M. Topič, Unique TiO₂ paste for high efficiency dye-sensitized solar cells, *Sol. Energy Mater. Sol. Cells* 93 (2009) 379–381.
- [17] F. Bella, G. Griffini, M. Gerosa, S. Turri, R. Bongiovanni, Performance and stability improvements for dye-sensitized solar cells in the presence of luminescent coatings, *J. Power Sources* 283 (2015) 195–203.
- [18] G. Griffini, F. Bella, F. Nisic, C. Dragonetti, D. Roberto, M. Levi, R. Bongiovanni, S. Turri, Multifunctional luminescent down-shifting fluoropolymer coatings: a straightforward strategy to improve the UV-light harvesting ability and long-term outdoor stability of organic dye-sensitized solar cells, *Adv. Energy Mater.* 5 (2015) 1401312.
- [19] S. Choi, E.-N.-R. Cho, S.-M. Lee, Y.-W. Kim, D.-W. Lee, Development of a high-efficiency laminated dye-sensitized solar cell with a condenser lens, *Opt. Express* 19 (2011) 818–823.
- [20] J.H. Kim, K.J. Moon, J.M. Kim, D. Lee, S.H. Kim, Effects of various light-intensity and temperature environments on the photovoltaic performance of dye-sensitized solar cells, *Sol. Energy* 113 (2015) 251–257.
- [21] K.J. Moon, S.W. Lee, Y.H. Lee, J.H. Kim, J.Y. Ahn, S.J. Lee, D.W. Lee, S.H. Kim, Effect of TiO₂ nanoparticle-accumulated bilayer photoelectrode and condenser lens-assisted solar concentrator on light harvesting in dye-sensitized solar cells, *Nanoscale Res. Lett.* 8 (2013) 283.
- [22] J.Y. Ahn, K.J. Moon, J.H. Kim, S.H. Lee, J.W. Kang, H.W. Lee, S.H. Kim, Designed synthesis and stacking architecture of solid and mesoporous TiO₂ nanoparticles for enhancing the light harvesting efficiency of dye-sensitized solar cells, *ACS Appl. Mater. Interfaces* 6 (2014) 903–909.
- [23] S.W. Lee, S.S. Lee, Shrinkage ratio of PDMS and its alignment method for the water level process, *Microsyst. Technol.* 14 (2008) 205–208.
- [24] T.-H. Kim, S.-H. Ha, N.-S. Jang, J. Kim, J.-H. Kim, J.-K. Park, D.-W. Lee, J. Lee, S.-H. Kim, J.-M. Kim, Simple and cost-effective fabrication of highly flexible, transparent superhydrophobic films with hierarchical surface design, *ACS Appl. Mater. Interfaces* 7 (2015) 5289–5295.
- [25] Y.-B. Park, H. Im, M. Im, Y.-K. Choi, Self-cleaning effect of highly water-repellent microshell structures for solar cell applications, *J. Mater. Chem.* 21 (2011) 633–636.
- [26] J.-H. Kong, T.-H. Kim, J. Kim, J.-K. Park, D.-W. Lee, S.-H. Kim, J.-M. Kim, Highly flexible, transparent and self-cleanable superhydrophobic films prepared by a facile and scalable nanopillar formation technique, *Nanoscale* 6 (2014) 1453–1461.